mass function of the brown dwarfs/giant planets, we need to conduct more comprehensive surveys for both types of (isolated and companion) ELL-YSOs. It is also important (*26*) to fill the gap between the very young brown dwarfs at several hundred astronomical units from their companions described in this paper and the close (0.5 to 10 astronomical units) extrasolar giant planets and brown dwarfs around nearby stars recently discovered (*27*).

References and Notes

1. T. Nakajima *et al.*, *Nature* **378**, 463 (1995); B. R. Oppenheimer, S. R. Kulkarni, K. Matthews, T. Nakajima, *Science* **270**, 1478 (1995); see also S. R. Kulkarni [*ibid.* **276**, 1350 (1997)] for a recent review of brown dwarfs.
2. R. Rebolo, M. R. Zapatero Osorio, E. L. Martin, *Nature* **377**, 129 (1995); M. R. Zapatero Osorio, R. Rebolo, E. L. Martin, *Astron. Astrophys.* **317**, 164 (1997); M. R. Zapatero Osorio, E. L. Martin, R. Rebolo, *ibid.* **323**, 105 (1997).
3. X. Delfosse *et al., Astron. Astrophys.* **327**, L25 (1997); J. D. Kirkpatrick, C. A. Beichman, M. F. Skrutskie, *ibid.* **476**, 311 (1997).
4. For possible theories on the formation of brown dwarfs, see P. Bodenheimer {in *Extrasolar Planets and Brown Dwarfs*, R. Rebolo *et al.*, Eds. [Astronomical Society of the Pacific (ASP) Conference Series 134, San Francisco, 1998], pp. 115–127} and F. C. Adams (*ibid.*, pp. 3–10).
5. Molecular cloud is the aggregation of interstellar gas and dust, being one of the coldest and densest components of the interstellar medium, where gas is mostly in the form of molecules.
6. M. Cohen and L. V. Kuhi, *Astrophys. J. Suppl.* **41**, 743 (1979); J. H. Elias, *Astrophys. J.* **224**, 857 (1978); C. Beichman *et al.*, *ibid.* **307**, 337 (1986); R. Neuhauser, M. Sterzik, J. Schmitt, R. Wichmann, J. Krautter, *Astron. Astrophys.* **295**, L5 (1995); L. Gauvin and K. M. Strom, *Astrophys. J.* **385**, 217 (1992).
7. Y. Itoh, M. Tamura, I. Gatley, *Astrophys. J.* **465**, L129 (1996).
8. F. Comeron, G. Rieke, A. Burrows, M. Rieke, *ibid.* **416**, 185 (1993); K. M. Strom, J. Kepner, S. E. Strom, *ibid.* **438**, 813 (1995).
9. L. Nordh *et al., Astron. Astrophys.* **315**, L185 (1996).
10. K. M. Strom, S. E. Strom, S. Edwards, S. Cabrit, M. Skrutskie, *Astron. J.* **97**, 1451 (1989).
11. C. Bertout, G. Basri, J. Bouvier, *Astrophys. J.* **330**, 350 (1988). It should be noted that thermal emission from disks might contribute to the *K*-band flux. This is the reason why we use the *J*-band and why we can discriminate YSOs from normal stars on the *J-H* versus *H-K* diagram.
12. The reddening corrections for the sources detected in this paper range from visual extinction of 0 to 10 magnitudes in Taurus and from 5 to 20 magnitudes in Chamaeleon. These values are consistent with the cloud extinction derived from $C^{18}O$ observations.
13. M. R. Meyer, N. Calvet, L. A. Hillenbrand, *Astron. J.* **114**, 288 (1997).
14. The reddening vector defines the direction and magnitude of the effect of extinction by the interstellar dust. This value is adapted from J. Koornneef [*Astron. Astrophys.* **128**, 84 (1983)].
15. The bolometric correction is from M. Bessel [*Astron. J.* **101**, 662 (1991)].
16. F. D'Antona and I. Mazzitelli, *Astrophys. J. Suppl.* **90**, 467 (1994). It should be noted that NIR photometry alone cannot uniquely determine both age and mass of the low-mass YSOs with these models. For the VLL-YSOs in Taurus (*7*), if we assume a younger age of 1 million years (Myr), a significant number of them are estimated to be substellar. However, at 10 Myr, only some VLL-YSOs are predicted to be substellar (see also Fig. 2).
17. Y. Itoh, M. Tamura, A. Tokunaga, in preparation.
18. K. L. Luhman, J. Liebert, G. H. Rieke, *ibid.* **489**, L165 (1997).
19. Y. Itoh, thesis, University of Tokyo (1998); Y. Itoh, M. Tamura, T. Nakajima, in preparation. These also include the coordinates and images of all the detected sources in Taurus (both YSOs and background sources).
20. Y. Oasa, M. Tamura, K. Sugitani, unpublished data.
21. Note that both the primary VLL-YSOs and the companions selected here show NIR colors consistent with those of YSOs with reddening by the cloud extinction. The NIR excesses suggest that both types of sources are YSOs with circumstellar structures and not simply background stars or galaxies projected within our region of observation by chance. It is also noteworthy that there is a similarity of the colors between the primary and secondary except for one pair as shown in Fig. 2A.
22. T. J. Jones, M. Ashley, A. R. Hyland, A. A. Ruelas-Mayorga, *Mon. Not. R. Astron. Soc.* **197**, 413 (1981).
23. J. P. Gardner, L. L. Cowie, R. J. Wainscoat, *Astrophys. J.* **415**, L9 (1993).
24. There will be two or three false $K < 18$ sources in 23 fields. In fact we detected two field star candidates within the same region (*19*), which were not listed in Table 1.
25. A. Burrows *et al., Astrophys. J.* **491**, 856 (1997); G. S. Stringfellow, *ibid.* **375**, L21 (1991).
26. M. Tamura *et al.*, in *Extrasolar Planets and Brown Dwarfs*, R. Rebolo *et al.*, Eds. (ASP Conference Series 134, San Francisco, 1998), pp. 338–341.
27. R. M. Mayor and D. Queloz, *Nature* **378**, 355 (1995); G. W. Marcy and R. P. Butler, *Astrophys. J.* **464**, L147 (1996).

28. Supported by Grant-in-Aid for Science Research of Japan. Infrared astronomy at Palomar was supported by a grant from the National Science Foundation. We thank K. Matthews and H. Suto for help with the observations. We also thank C. Packham and M. Merrill for reading the manuscript.

5 June 1998; accepted 6 October 1998

Ages of Prehistoric Earthquakes Revealed by Cosmogenic Chlorine-36 in a Bedrock Fault Scarp at Hebgen Lake

Marek Zreda and Jay S. Noller

Cosmogenic chlorine-36 reveals dates of the multiple prehistoric earthquakes that have produced a scarp on the Hebgen Lake fault. Apparent chlorine-36 ages are stratigraphically correct, follow a predicted theoretical pattern, and produce geologically reasonable model ages of 24, 20, 7.0, 2.6, 1.7, and 0.4 thousand years ago. This result demonstrates the feasibility of using cosmogenic chlorine-36 to extract paleoearthquake records from bedrock fault scarps.

Verification of long-term earthquake models with field observations requires records that contain multiple, well-dated earthquakes. However, such paleoseismic records are rare because landforms and sediments that record faulting are difficult to identify and are easily buried or eroded; commonly, evidence of earlier earthquakes is obscured by later ones (*1*). Bedrock fault scarps are the best evidence of past earthquakes. They are clearly associated with a particular fault, they frequently record multiple earthquakes, and they tend to remain unmodified because of their resistance to erosion. A major past disadvantage of bedrock fault scarps is that they have not been datable by numerical techniques with adequate precision and accuracy (*2*). Here, we describe an approach to dating prehistoric earthquakes based on the buildup of cosmogenic ^{36}Cl in bedrock scarps exposed during surface faulting, and discuss its application to a limestone scarp on the Hebgen Lake fault (*3, 4*), Montana (Fig. 1). The technique measures how long the different, episodically offset parts of the scarp have been exposed to cosmic radiation.

M. Zreda, Department of Hydrology and Water Resources, University of Arizona, Tucson, AZ 85721, USA. J. S. Noller, Department of Geology, Vanderbilt University, Nashville, TN 37235, USA.

Cosmogenic ^{36}Cl is produced by cosmic-ray neutrons and muons that interact with ^{39}K, ^{40}Ca, and ^{35}Cl in materials in the top few meters of Earth's crust (*5–7*). Because the production rate of ^{36}Cl (*7, 8*) and its distribution below the surface (*9, 10*) are known, the concentration of cosmogenic ^{36}Cl can be used to calculate how long a surface has been exposed to cosmic radiation, that is, to determine its surface exposure age. In the case of a fault scarp, the cosmogenic ^{36}Cl exposure age is the time since the scarp face was suddenly exposed during a large surface-faulting earthquake.

Before faulting, only a small amount of cosmogenic ^{36}Cl accumulates below the surface because of shielding by the overlying rocks. In limestones, this subsurface production is dominated by spallation of ^{40}Ca at depths of <3 m and by negative muon capture by ^{40}Ca below that depth (*11*). At a depth of 2 m, the total production rate due to spallation and negative muon capture decreases to <10% of that at the surface. This inherited component of ^{36}Cl can be quantified and subtracted from the total measured ^{36}Cl to determine the surface exposure age of the fault scarp, and thus the age of the earthquake. In a scarp representing multiple earthquakes, then, concentrations of ^{36}Cl will gradually increase from a minimum at the bottom of the face and change abruptly at places representing different slip events (Fig. 2). A sufficient number of samples must be collected to resolve this spatial and temporal pattern of accumulated ^{36}Cl.

We examined a scarp in limestone of the Middle Cambrian Meagher Formation (*12*) on the Hebgen Lake fault. The last large earthquake (1959, M_s = 7.5) (*3*) produced surface ruptures 34 km long with vertical offsets of up to 6.5 m. On a >12-m-high fault scarp in limestone bedrock, we identified the 2.1-m-high 1959 face and older, progressively more weathered faces toward the top. We collected 21 samples, every ~0.5 m, from 0.5 m to >10 m above the bottom of the youngest pre-1959 scarp. In addition, we collected six samples from the freshly exposed 1959 face. The samples were collected, processed, and analyzed using standard methods (*13*), and apparent ^{36}Cl ages were calculated (*14*).

Apparent ^{36}Cl ages (those not corrected for ^{36}Cl accumulation below the surface) increase from near zero at the bottom of the scarp to 37,000 years ago (37 ka) at the top (Fig. 3A) (*15*). With one exception, these ages are in correct stratigraphic order. They form a pattern similar to that predicted by our conceptual model (Fig. 2), with six different sections that correspond to faces exposed by separate earthquakes. These sections have been recognized in the field on the basis of surface characteristics: smoothness, preservation of polish (slickensides), degree of surface pitting, and coloration. The 1959 surface (section 1 in Fig. 3A) is smooth, highly polished, heavily mineralized, and light brown. Lower (younger) pre-1959 faces have a fresh, smooth, unweathered appearance, contain well-preserved (section 2) or slightly weathered (section 3) slickensides, and are light beige and gray. Upper (older) faces have progressively deeper and wider weathering pits. Section 4 has parallel weathering grooves developed along former slickensides. Section 5 has deep weathering pits with no recognizable directional pattern; any former slickensides have been completely obliterated by weathering. The uppermost part (section 6) is similar to section 5 in surface weathering, but it is clearly distinguishable by its much darker color.

Model ages of paleoearthquakes (Fig. 3B) are calculated by correcting the apparent ages for ^{36}Cl that accumulated below the surface before the rupture that exposed the face, in accord with the conceptual model of scarp exposure and accumulation of cosmogenic ^{36}Cl. In the calculations of model ages, geochemical and isotopic data are used together with the locations of the weathering boundaries determined in the field. The data imply that earthquakes occurred 0.4, 1.7, 2.6, 7.0, 20.3, and 23.8 ka. All six model ages are statistically different at the 1σ level (Fig. 3B). However, at the 2σ level, there are overlaps in groups 6 and 5, 3 and 2, and 2 and 1. This resolution problem is due to the short time intervals between earthquakes, combined with difficulties in measuring the extremely low concentrations of stable Cl in the samples (*15*). An independent age estimate of 2.8 ± 1.1 ka has been obtained for a pre-1959 scarp

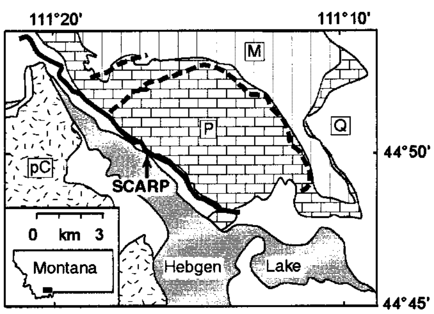

Fig. 1. Location of the bedrock scarp that was dated using cosmogenic ^{36}Cl (pC, Precambrian; P, Paleozoic; M, Mesozoic; Q, Quaternary). Thick line shows the 1959 surface rupture (solid line, Hebgen Lake fault; dashed line, other faults). The coordinates at the bottom of the scarp are 44.834°N, 248.723°E, 2027 m above sea level.

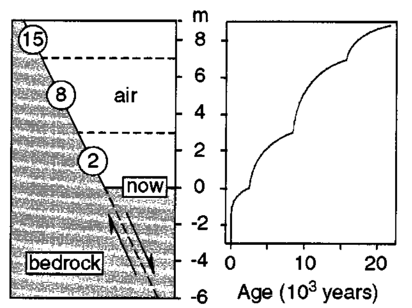

Fig. 2. Accumulation of cosmogenic ^{36}Cl in a hypothetical fault scarp formed by three earthquakes that occurred at 15, 8, and 2 ka. Cosmogenic ^{36}Cl ages form a characteristic pattern: exponential decrease with depth within each section of the scarp, and abrupt changes in the slope at boundaries between sections exposed at different times.

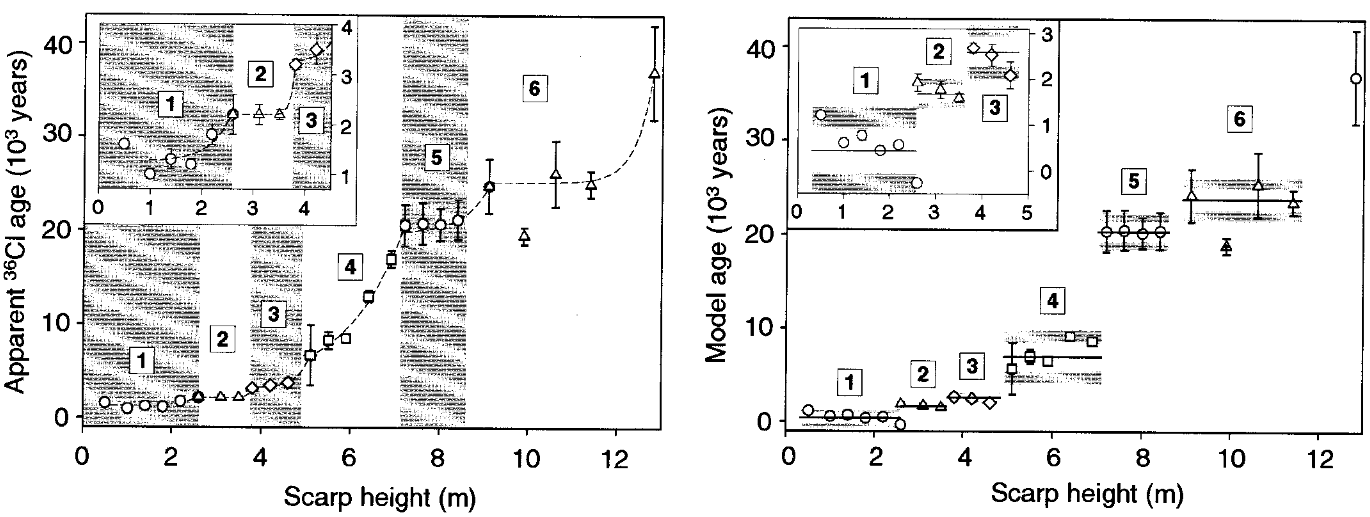

Fig. 3. Cosmogenic ^{36}Cl ages for the bedrock scarp on the Hebgen Lake fault. Group 1 is from the 1959 scarp; groups 2 through 6 are from the pre-1959 part of the scarp, ~20 m east of group 1. Sections 1 through 6 have been defined in the field using the degree of surface weathering and coloration. Individual apparent ages (left panel) form a pattern expected for scarps formed by recurring faulting. Error bars (1 SD) represent overall analytical uncertainty calculated using Monte Carlo simulation. Exponential best fits (dashed lines) delineate a trend within each group, similar to that predicted by the conceptual model (Fig. 2). Model ages (right panel) form six groups whose means (solid lines) are statistically different at the 1σ level (white bands). At the 2σ level (gray bands), groups 5 and 6, 2 and 3, and 1 and 2 are statistically indistinguishable. These parts of the scarp are considered to have been formed by different earthquakes, on the basis of differences in surface appearance.

~10 km to the south from slope diffusion modeling (*16*). This age agrees within uncertainty with our age of 2.6 ka.

Our results indicate that most of the slip occurred at ~24 to 20 ka and 7 to 0 ka. These times of increased activity were separated by a period of relative seismic quiescence. A similar time interval separates the period of activity at 20 to 24 ka from the next older ^{36}Cl age of ~37 ka, suggesting that earthquake activity on the Hebgen Lake fault is periodic. This temporal clustering of paleoearthquakes is similar to that described elsewhere for the Great Basin (*17, 18*) and suggested for other intraplate faults (*19*).

References and Notes

1. J. P. McCalpin, Ed., *Paleoseismology*, vol. 62 of *International Geophysics Series* (Academic Press, San Diego, CA, 1996).
2. J. S. Noller, J. M. Sowers, W. R. Lettis, Eds., *Quaternary Geochronology: Applications in Quaternary Geology and Paleoseismology* (American Geophysical Union, Washington, DC, in press).
3. W. B. Myers and W. Hamilton, *U.S. Geol. Surv. Prof. Pap. 435*, 58 (1964).
4. I. J. Witkind, *ibid.*, p. 37.
5. R. Davis Jr., and O. A. Schaeffer, *Ann. N.Y. Acad. Sci.* **62**, 105 (1955).
6. F. M. Phillips, B. D. Leavy, N. O. Jannik, D. Elmore, P. W. Kubik, *Science* **231**, 41 (1986).
7. M. G. Zreda *et al.*, *Earth Planet. Sci. Lett.* **105**, 94 (1991).
8. F. M. Phillips, M. G. Zreda, M. R. Flinsch, D. Elmore, P. Sharma, *Geophys. Res. Lett.* **23**, 949 (1996).
9. B. Liu, F. M. Phillips, J. T. Fabryka-Martin, M. M. Fowler, R. S. Biddle, *Water Resour. Res.* **30**, 3115 (1994).
10. J. O. H. Stone, J. M. Evans, L. K. Fifield, G. L. Allan, R. G. Cresswell, *Geochim. Cosmochim. Acta* **62**, 433 (1998).
11. J. T. Fabryka-Martin, thesis, University of Arizona (1988).
12. R. G. Tysdal, *Geologic Map of the Sphinx Mountain Quadrangle and Adjacent Parts of the Cameron, Cliff Lake, and Hebgen Dam Quadrangles, Montana* (I-1815, U.S. Geological Survey, Washington, DC, 1990).
13. Rock samples were collected from top 2 to 5 cm of rock using hammer and chisel. The samples were cleaned of any organic material and encrustations, crushed and ground, and sieved to size fraction 0.25 to 1.00 mm. To remove any meteoric ^{36}Cl, they were leached first in 3% nitric acid for a few minutes and then in deionized water for 24 hours, dried in an oven overnight at 100°C, and placed in sterile plastic bags. Samples for ^{36}Cl were obtained by dissolution of 100 g of purified rocks in sufficient amount of 5% nitric acid mixed with 20 ml of 0.1 M $AgNO_3$. To prevent rapid sample dissolution and minimize possible loss of Cl with released CO_2, nitric acid was dispensed slowly (1 ml/min) using a pump. Chloride was precipitated as AgCl (*12*) [M. G. Zreda, F. M. Phillips, S. S. Smith, *Cosmogenic ^{36}Cl Dating of Geomorphic Surfaces* (*Hydrology Program Rep*. 90-1, New Mexico Institute of Mining and Technology, 1990); M. G. Zreda, thesis, New Mexico Institute of Mining and Technology (1994)], which was rinsed in deionized water and purified of sulfur with barium nitrate. Chlorine-36 was measured by accelerator mass spectrometry [D. Elmore *et al.*, *Nature* **277**, 22 (1979)] at Purdue University. Major elements were determined by x-ray fluorescence or inductively coupled plasma–atomic emission spectrometry, and Cl by the ion-selective electrode method [P. J. Aruscavage and E. Y. Campbell, *Talanta* **30**, 745 (1983)] modified for carbonate rocks.
14. Apparent cosmogenic ^{36}Cl surface exposure ages were calculated using CHLOE software [F. M. Phillips and M. A. Plummer, *Radiocarbon* **38**, 98 (1996)], with spallation production rates of 73.3 ± 4.9 atoms ^{36}Cl (g Ca)$^{-1}$ year^{-1} and 154 ± 10 atoms ^{36}Cl (g K)$^{-1}$ year^{-1} (*8*) and thermal neutron activation production rate calculated (*9*) from the fast neutron production rate of 586 ± 40 neutrons (g air)$^{-1}$ year^{-1} (*8*). We used these production rates because they were determined from a large number of samples of different ages and from 15 separate locations; other production rate studies used single locations or small numbers of samples. These production rates are for sea level and high latitudes and were scaled [D. Lal, *Earth Planet. Sci. Lett.* **104**, 424 (1991)] to the locations of sample sites. In addition, we accounted for muogenic production (*10*) below the surface and for topographic shielding by the scarp [M. G. Zreda and F. M. Phillips, in *Dating in Exposed and Surface Contexts*, C. Beck, Ed. (Univ. of New Mexico Press, Albuquerque, 1994), pp. 161–183]. We did not correct the production rates for temporal variability because doing so does not improve the uncertainty of the production rate estimates (*8*). Uncertainties of the ^{36}Cl ages are due to a combination of analytical errors and systematic errors associated with production rate calculations. These uncertainties are <15% for moraines from which multiple rock samples per surface are analyzed [F. M. Phillips *et al.*, *Geol. Soc. Am. Bull.* **109**, 1453 (1997)]. Two additional sources of systematic error are related to production of ^{36}Cl below the surface and to topographic shielding by the scarp. The errors associated with these variables are not well known, but they are likely on the order of 10%.
15. See *Science* Online (www.sciencemag.org) for supplementary data on sample heights, ^{36}Cl production parameters, and cosmogenic ^{36}Cl ages for six different sections of the Hebgen fault scarp.
16. D. B. Nash, *Geol. Soc. Am. Bull.* **95**, 1413 (1984).
17. R. E. Wallace, *J. Geophys. Res.* **89**, 5763 (1984).
18. ———, *Seismol. Soc. Am. Bull.* **74**, 301 (1987).
19. A. J. Crone and K. V. Luza, *Geol. Soc. Am. Bull.* **102**, 1 (1990).

20. Supported by the Nuclear Regulatory Commission, the Packard Fellowship in Science and Engineering, and NSF. We thank W. Lettis for field assistance, R. Schapiro and D. Robinson for help in sample collection, and two anonymous reviewers for constructive comments.

2 July 1998; accepted 7 October 1998

Detection of Centimeter-Sized Meteoroid Impact Events in Saturn's F Ring

Mark R. Showalter

Voyager images reveal that three prominent clumps in Saturn's F ring were short-lived, appearing rapidly and then spreading and decaying in brightness over periods of ~2 weeks. These features arise from hypervelocity impacts by ~10-centimeter meteoroids into F ring bodies. Future ring observations of these impact events could constrain the centimeter-sized component of the meteoroid population, which is otherwise unmeasurable but plays an important role in the evolution of rings and surfaces in the outer solar system. The F ring's numerous other clumps are much longer lived and appear to be unrelated to impacts.

The faint and narrow F ring orbits 3000 km beyond the outer edge of Saturn's main ring system. It was discovered during the Pioneer 11 encounter in 1979 (*1*) but was imaged more clearly and extensively by Voyager's cameras in 1980 and 1981 (*2*, *3*). The Voyager images revealed a variety of peculiar structures within the ring, variously described as strands, kinks, clumps, and "braids." Many of these structures are now believed to be related to gravitational perturbations by the nearby "shepherding" moons Prometheus and Pandora (*4–6*), but details of the interactions remain mysterious.

The F ring appears much brighter in forward-scattered than backscattered light, suggesting diffraction by a population of fine dust. Photometric models reveal the dust to be predominantly <1 μm in size (*7*). Such fine dust has a brief lifetime of 10^3 to 10^6 years against various drag forces and loss mechanisms (*8*), so it must be replenished by an unseen population of larger parent bodies.

After Voyager, the F ring was not seen again until 1995, during the crossings of Earth and sun through Saturn's ring plane. Observers reported a number of new moons near the F ring (*9–11*); however, with implied radii of ~10 km, these bodies were too large to have escaped detection by Voyager. They have integrated brightnesses comparable to that of the brightest clumps observed by Voyager (*10*), so clumps provide a much more plausible explanation for these "moons." The numbers and locations of the clumps changed between observations in May, August, and November of 1995 (*9–11*), suggesting that they are transient, with lifetimes <3 months.

The 1995 images provided a firmer constraint than the Voyager data set, which merely showed that no major clumps survived for the ~9 months between encounters (*12*). However, the Voyager data set is much more extensive than any obtainable from the ground, with reasonable resolution and nearly complete longitudinal coverage for periods of

Space, Telecommunications and Radioscience Laboratory, Stanford University, Stanford, CA 94305, USA. Mailing address: 245-3 NASA Ames Research Center, Moffett Field, CA 94035–1000, USA. E-mail: showalter@ringside.arc.nasa.gov